

Decadal and Multidecadal North Atlantic SST Anomalies Driven by Standing and Propagating Basin-Scale Atmospheric Anomalies

GEORGE R. HALLIWELL JR.

MPO/RSMAS, University of Miami, Miami, Florida

(Manuscript received 15 September 1995, in final form 1 August 1996)

ABSTRACT

North Atlantic winter surface atmospheric circulation anomalies that vary over decadal and longer periods are characterized by examining the life history of individual anomaly features present from 1950 to 1992. Individual features observed on surface pressure anomaly (PA) maps propagated to the east-northeast during the early to mid-1950s and to the south from 1964 to 1984. Standing PA fluctuations were observed at other times. The nonstationary statistical properties of this atmospheric variability were not apparent in earlier studies because the statistical analysis techniques used assumed stationarity or assumed the atmosphere was dominated by standing patterns of variability. Observed winter sea surface temperature anomaly (SSTA) patterns that vary over decadal and longer periods were driven in part by these surface atmospheric anomalies through the associated anomalous surface turbulent heat flux patterns. The ocean tends to be anomalously cold (warm) where the surface wind speed is anomalously large (small). Local atmospheric forcing of winter SSTA remains important out to longer periods than previously realized. Although SSTA appears to respond passively to this atmospheric forcing, a complete understanding of the ocean-atmosphere variability documented here will require an understanding of processes responsible for driving the atmospheric circulation anomalies.

1. Introduction

Energetic interannual sea surface temperature anomaly (SSTA) variability observed in the North Atlantic Ocean plays an important role in climate. SSTA influences the exchange of heat and mass between the atmosphere and ocean, and also influences the exchange of properties between the upper-ocean mixed layer and the deeper ocean. In the North Atlantic, persistent SSTA patterns are related to persistent anomalous patterns of atmospheric pressure, wind, temperature, and precipitation over the ocean and adjacent continents (e.g., Folland et al. 1986; Lau and Nath 1990; Zorita et al. 1992). SSTA patterns that vary over periods of a few decades are driven to a large extent by changes in Atlantic Ocean circulation (e.g., Bjerknes 1964), both the wind-driven gyre circulation and the meridional overturning circulation. In contrast, interannual SSTA fluctuations with periods close to and shorter than decadal are primarily driven locally by the atmosphere through anomalous air-sea fluxes (e.g., Bjerknes 1964; Kushnir 1994; Halliwell and Mayer 1996).

Previous studies have not provided a clear picture of how SSTA is driven at timescales characteristic of the

transition between atmospheric and oceanic forcing, in particular for the energetic SSTA variability observed within the North Atlantic westerly wind belt. Modeling studies have suggested that internal ocean circulation oscillations may be responsible for SSTA variability in this region (e.g., Weaver and Sarachik 1991; Delworth et al. 1993; Greatbatch and Zhang 1995). In contrast, Halliwell and Mayer (1996) demonstrated that winter SSTA variability in this region with periods of 10–20 yr responds substantially to forcing by the anomalous surface turbulent heat flux arising from anomalous wind speed variability. Further questions were raised by the analysis of Hansen and Bezdek (1996), who described the life history of several large-scale winter SSTA features present in the North Atlantic between 1948 and 1992 that had individual life spans of 3–12 yr. Some of these features propagated in the general direction of the oceanic flow, but often at a speed substantially slower than the expected flow speed. Since previous studies have documented a characteristic SSTA decay timescale of about 3 months in the North Atlantic (Reynolds 1979; Frankignoul and Reynolds 1983; Frankignoul 1985; Halliwell and Mayer 1996), the anomalous forcing must also persist to maintain these SSTA features against dissipation. Due to the short timescales characteristic of internal atmospheric variability, it is tempting to conclude that oceanic forcing maintains these SSTA features. The results of Halliwell and Mayer (1996), however, suggest that local air-sea flux anomalies could maintain them.

Corresponding author address: Dr. George R. Halliwell, RSMAS/MPO, University of Miami, 4600 Rickenbacker Causeway, Miami, FL 33149-1098.
E-mail: grh@palm.rsmas.miami.edu

The present analysis is designed to verify the importance of local atmospheric forcing over timescales characteristic of the transition between atmospheric and oceanic forcing (periods of 10–40 yr). This is achieved by first characterizing properties of the atmospheric circulation anomalies that vary over these long timescales. The life histories of individual atmospheric anomaly features are examined using a time series of winter anomalous surface pressure (PA) maps. This simple examination reveals properties that were obscured in earlier studies due to the analysis techniques that were used. It is then demonstrated that a substantial fraction of decadal and longer-period North Atlantic winter SSTA variability is driven by these atmospheric anomalies, largely through the associated anomalous surface heat flux pattern. The analysis is performed using monthly SST and surface pressure maps for 1950 through 1992 obtained from the Comprehensive Ocean–Atmosphere Data Set (COADS; Woodruff et al. 1987). Preliminary processing of these data is described in Mayer and Weisberg (1993). The PA and SSTA maps analyzed here were generated by averaging January through March maps for each year, then subtracting mean winter pressure and SST from each set of maps. Both sequences of winter maps were then temporally filtered using four passes of a three-point von Hann window at each grid point to emphasize variability with decadal and longer periods.

2. Decadal and multidecadal winter PA anomalies

Thirty of the 43 temporally filtered winter PA maps from 1950 to 1992 are plotted in Fig. 1 to illustrate the evolution of the five high pressure anomalies (H1 through H5) and three low pressure anomalies (L1 through L3) that dominated decadal and longer-period winter PA variability. During the winter of 1951, most of the North Atlantic was dominated by a strong high pressure anomaly feature (H1). The highest anomalous pressure of nearly 4 hPa was located in the central part of the basin, between 40° and 50°N. Over the next few years, H1 propagated to the east-northeast as it gradually weakened, reaching the British Isles by the mid-1950s. From the late 1950s through the mid-1960s, propagation was no longer evident in the PA field. Instead, a large anomalous low pressure region (L1) formed and gradually strengthened to the north of 30°N, with the anomaly magnitude in the central basin between 45° and 50°N exceeding 3.5 hPa by 1965. Anomalous high pressure (H2) was present south of L1 from 1959 to 1963.

Beginning in 1964 and continuing to 1984, basin-scale winter PA features (Fig. 1) apparently propagated from north to south. This propagation is more clearly illustrated in a time–latitude plot of zonally averaged PA (Fig. 2) and involves PA features L1, H3, L2, and H4. The dominant period of these propagating PA features was about 12 yr, and they rapidly decayed as they propagated to the south of 30°N. Anomalous surface

pressure features often propagated southward at a rate of about 10° latitude per year, but individual features sometimes slowed down for 2–3-yr intervals, such as H3 during 1971 and 1972. Southward propagation ceased after 1984. Beginning in 1988, a strong high pressure anomaly (H5) formed over the central and northeastern part of the analysis domain, while low pressure (L3) formed to the north and northwest of H5. The PA patterns of the early 1990s resemble the patterns present in the early to mid-1950s, suggesting the existence of PA variability with periods near 40 yr.

The nonstationary statistical properties of PA variability summarized here, in particular the propagation of some PA features, were obscured in earlier studies. This resulted because statistical analysis techniques (e.g., time-domain EOFs and difference maps between selected years) that resolved standing patterns of variability and that assumed that the variability was statistically stationary were generally used (e.g., Bjerknes 1964; Wallace et al. 1992; Zorita et al. 1992; Deser and Blackmon 1993; Kushnir 1994).

3. Winter SSTA response to the atmospheric circulation anomalies

Examination of the sequence of filtered winter SSTA maps from 1950 to 1992 revealed that a substantial fraction of SSTA variability was related to the atmospheric circulation anomalies in Fig. 1 (not shown). In general, the ocean tended to be anomalously cold (warm) wherever the PA features acted to make the wind stronger (weaker) than normal. This relationship is illustrated in the SSTA maps for 1951 and 1955 (Fig. 3), a time interval in which PA feature H1 was observed to propagate east-northeastward (Fig. 1). The basin-scale, zonally banded SSTA pattern present during 1951 can be qualitatively related to the wind anomaly pattern associated with H1. During 1951, the existence of H1 resulted in anomalously strong westerlies north of 45°–50°N, a region in which SST was anomalously cold. Between 30° and 45°–50°N, H1 resulted in anomalously weak westerlies and anomalously warm SST. From 10°–30°N, H1 resulted in anomalously strong trade winds and anomalously cold SST.

The warm anomaly region present in the southern part of the westerlies during 1951 is of particular interest. The two SSTA maxima associated with this anomaly (W1 and W2) are labeled in Fig. 3, as is the location of the center of PA feature H1. Both W2 and H1 propagated east-northeastward at about the same speed between 1951 and 1955 (Fig. 3) so that the warm anomaly remained to the south and southwest of the center of H1, where the westerlies were abnormally weak. The coexistence and copropagation of these features is suggestive of a coupled ocean–atmosphere phenomenon—that is, the anomalous wind pattern associated with H1 maintaining W2 and the anomalous atmospheric heating pattern associated with W2 maintaining H1. Advection

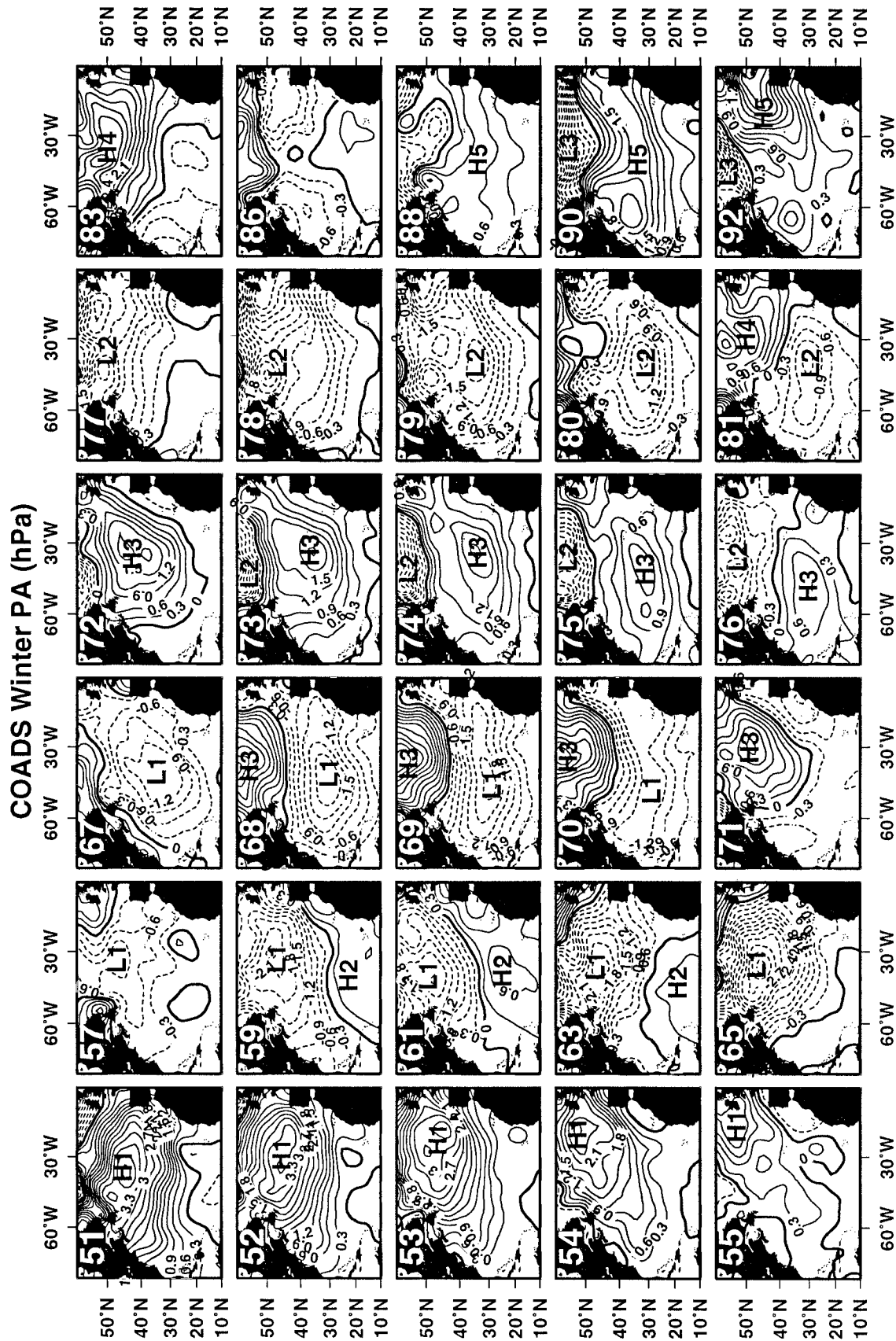


FIG. 1. Fields of winter surface atmospheric pressure anomaly calculated by removing the climatological winter mean from COADS surface atmospheric pressure fields. Thirty of the 43 yr between 1950 and 1992 are shown; the years were subjectively selected to maintain the continuity of individual anomaly features. Anomalous high pressure features H1 through H5 and low pressure features L1 through L3 are labeled. Dashed contours indicate negative anomalies.

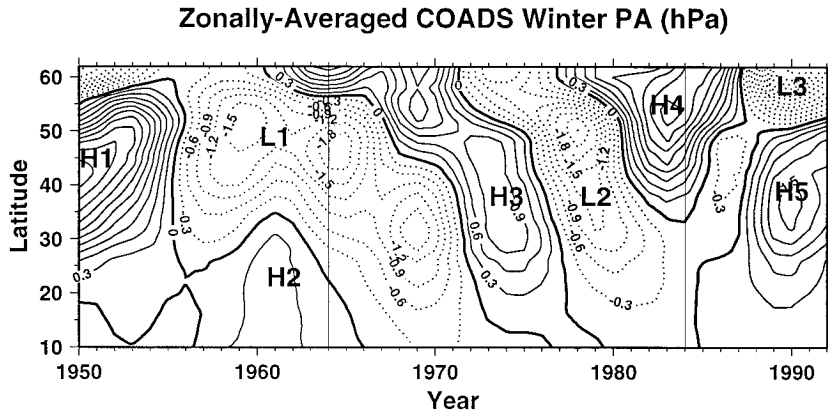


FIG. 2. Time–latitude plot of zonally averaged PA calculated from the temporally filtered maps in Fig. 1. The anomalous PA features labeled in Fig. 1 are also labeled here. Vertical lines delineate the 2 decades in which PA features propagated southward. Dashed contours indicate negative anomalies.

of W2 by the oceanic flow field may contribute to the observed propagation. Although coupling cannot be proven here, the H1–W2 pair has a timescale of decay of several years, much longer than characteristic atmospheric timescales and the SSTA timescale of decay.

Halliwell and Mayer (1996) decomposed dependent variables in the bulk formula representation of anomalous surface turbulent (sensible plus latent) heat flux

into mean annual cycle (superscript *) and anomaly (subscript *a*) components. They demonstrated that anomalous wind speed significantly influenced North Atlantic winter SSTA variability, primarily through the following component of this heat flux:

$$QTA = \rho_a W_a [C_s(\delta T)^* + C_L L(\delta q)^*], \quad (1)$$

where ρ_a is the air density, W_a is the anomalous wind speed, C_s and C_L are bulk coefficients, L is the latent heat of evaporation, and $(\delta T)^*$ and $(\delta q)^*$ are the climatological mean annual cycles of sea–air temperature and specific humidity differences. Heat flux is assumed to be positive upward. COADS fields of W_a in conjunction with COADS climatologies of $(\delta T)^*$ and $(\delta q)^*$ were used to calculate winter fields of QTA, and then the sequence of winter QTA maps was temporally filtered for comparison to PA and SSTA.

To efficiently compare forcing patterns estimated from (1) to SSTA patterns, changes that occurred between “antinodes” of atmospheric variability were examined for two cases. The first case focuses on the changes that occurred from 1952 to 1965. Anomalous surface pressure features H1 in 1952 and L1 in 1965 are nearly identical in structure and location, but opposite in sign (Fig. 1). The second case focuses on antinodes of the southward-propagating PA features present between 1964 and 1984. The years 1968 and 1980 are selected to represent one phase of this variability, while 1974 is selected to represent the opposite phase (Fig. 1). The analysis for both cases is presented in Fig. 4.

From 1952 to 1965, pressure fell in the North Atlantic between 20° and 60°N, and the largest decrease of 7 hPa was found in midbasin near 45°N (Fig. 4). This change pattern is consistent with a southward displacement of both the subtropical high and the subpolar (Icelandic) low. The map of the associated change of QTA from 1952 to 1965 displays a zonally banded structure similar to the observed change of SSTA, but with pos-

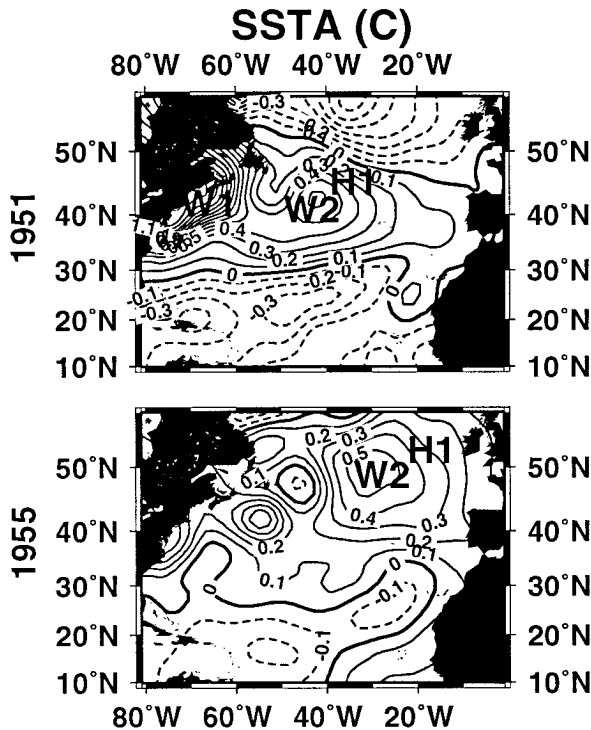


FIG. 3. Temporally filtered SSTA maps for 1951 and 1955. Warm anomaly centers W1 and W2 are labeled. The central location of PA feature H1 (Fig. 1) is labeled in both panels. Dashed contours indicate negative anomalies.

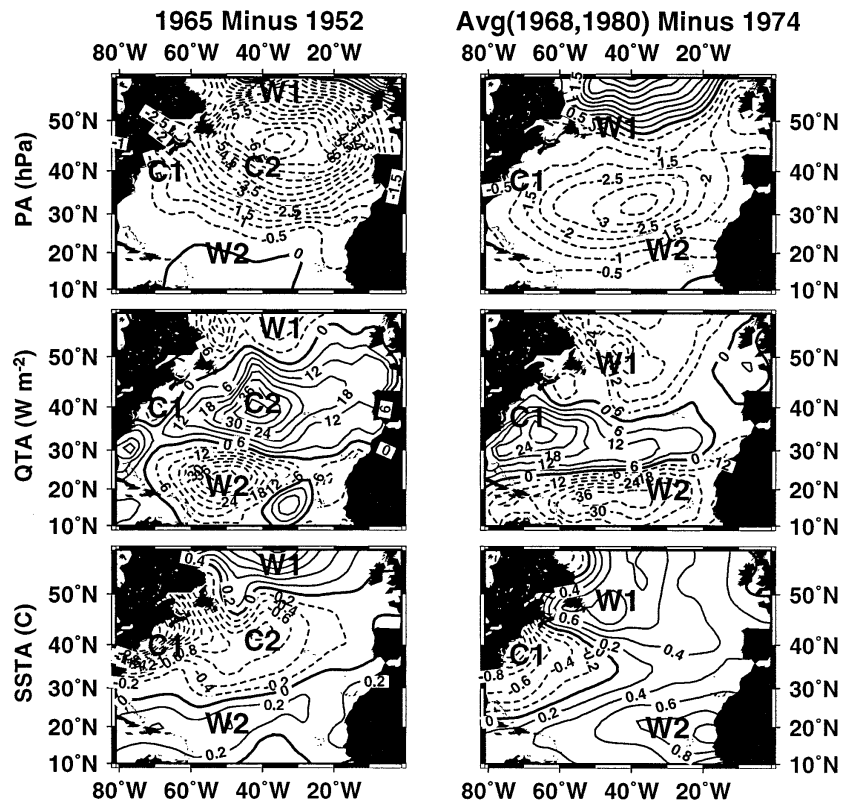


FIG. 4. Analysis of difference patterns in PA, QTA from (1), and SSTA for two cases: the change from 1952 to 1965 (left) and the difference between the average of the 1968 and 1980 fields minus the 1974 fields. Centers of SSTA warming and cooling from the bottom panels are labeled in all three panels for each case.

itive (upward) QTA corresponding to negative SSTA (Fig. 4). SSTA warmed north of 50°N (region W1) where the westerlies weakened, cooled between 30° and 50°N (regions C1 and C2) where the westerlies strengthened, and warmed south of 30°N (region W2) where the trade winds weakened. The patterns of QTA and SSTA change are not expected to be identical because processes other than QTA influence SSTA and also because the COADS-derived fields contain significant errors. The cooling observed in region C1 is not explained by the change in QTA. Since this region is located off the east coast of North America, it will be strongly influenced by surface heat flux anomalies resulting from atmospheric temperature and humidity anomalies (which are not included in QTA), especially those due to winter cold air outbreaks. It will also be influenced by anomalous thermal advection associated with Gulf Stream variability. Over the open ocean, however, the basin-scale patterns of QTA and SSTA are reasonably similar and verify the significant influence of the PA features in Fig. 1 on SSTA. Since this change represents variability with a half-period of 13 yr, forcing by the PA features in Fig. 1 can extend to periods substantially longer than decadal.

Concerning opposite phases of the southward-prop-

agating PA pattern present from 1964 to 1984, the years 1968 and 1980 represent a low North Atlantic oscillation (NAO) index pattern (e.g., Hurrell 1995). During these 2 yr, the subtropical high and Icelandic low were both anomalously weak (Fig. 1), leading to a relatively small pressure difference (low index) between these pressure centers. In contrast, the year 1974 represents the opposite phase of this PA pattern and thus a high NAO index. Changes that occurred in going from a high to a low NAO index are illustrated in Fig. 4 by subtracting the 1974 PA, QTA, and SSTA fields from the averages of the 1968 and 1980 fields. The resulting PA difference pattern (Fig. 4) reveals the decrease in pressure over the subtropical high (exceeding 3.5 hPa) and the increase in pressure over the Icelandic low. It is similar to the PA change pattern from 1952 to 1965, but displaced about one-quarter of a meridional wavelength to the south. Because the PA difference pattern for low minus high NAO index years is generally associated with a simultaneous decrease in the strength of the westerlies and the trades, the open ocean warms in both the westerlies (region W1) and the trades (region W2; Fig. 4). In contrast to the open ocean, the ocean is colder in the western subtropical gyre off the coast of North America (region C1) during low index years.

The QTA pattern related to the change in NAO index displays a basin-scale pattern similar to that of SSTA but of opposite sign, not only including the open ocean, but also including the cooling region C1 off the North American coast. SSTA cooling associated with C1 tends to extend eastward along 30°–35°N, in part due to a narrow zonal band of relatively strong westerlies and, hence, positive QTA. QTA cannot account for the strongest warming in the trade wind belt (W2) being found off the African coast. Clouds, coastal upwelling, and atmospheric humidity have a large influence on SSTA in this region. The presence of warm (cold) SSTA in the westerlies during low (high) NAO index years has been documented in earlier studies (e.g., Cayan 1992). What emerges from the present study is that at decadal and longer periods, fluctuations in the NAO index are not necessarily the result of standing pressure oscillations.

4. Discussion

Although modeling studies have demonstrated the importance of internal oceanic circulation oscillations in driving SSTA variability at periods exceeding decadal, present results demonstrate that local atmospheric forcing cannot be neglected in comparison to these oceanic forcing mechanisms over periods of up to 20–30 yr. The importance of atmospheric forcing was demonstrated by following the life history of individual winter PA features that vary over decadal and longer periods, and then relating observed winter SSTA patterns to these atmospheric anomaly features. An accurate simulation of this locally forced SSTA variability will be required to unambiguously identify the SSTA response to oceanic forcing, in particular to changes in the meridional overturning circulation. The PA anomaly features responsible for driving decadal and longer SSTA variability have basin scales and highly nonstationary statistical properties. In particular, propagation of PA features was observed during part of the 42-yr study interval, east-northeastward during the early and mid-1950s and southward from 1964 to 1984. We cannot entirely rely on statistical analysis techniques that assume atmospheric and oceanic variability are stationary and consist of standing patterns of oscillation.

Although atmospheric forcing of SSTA variability has been established, this is only part of the story. We must determine how the PA features responsible for driving SSTA are forced to fully understand how the atmosphere and ocean are coupled at decadal and longer periods. As an example, a high pressure anomaly H1 and a warm SSTA feature W2 [which was one of the major propagating anomaly features observed by Hansen and Bezdek (1996)] propagated together toward the east-northeast during the early and mid-1950s (Fig. 3), suggesting that they may be coupled. Although the warm SSTA feature was maintained in part by the relatively weak westerlies to the south and southwest of

H1, could the warm anomaly feature have been at least partly responsible for maintaining H1? [Hansen and Bezdek (1996) did not attempt to relate the observed warm SSTA feature to anomalous surface turbulent heat flux forcing.] Palmer and Sun (1985) forced an atmospheric model with imposed Atlantic SST and demonstrated that warm SST in the western North Atlantic over a large region centered to the south and southeast of Newfoundland (roughly the region occupied by warm anomaly W2 in the early 1950s; Fig. 3) acted to shift the jet stream and storm track to the north over the Atlantic basin. This shift resulted in anomalously high surface pressure over the North Atlantic. However, the center of this high surface pressure was located in the eastern North Atlantic and not to the northeast of the warm anomaly center, as was observed for the W2–H1 pair in Fig. 3. A fully coupled model may be required to reproduce the observed W2–H1 relationship.

One consideration in determining to what extent SSTA patterns contribute to maintaining the PA features in Fig. 1 is that PA features present during summer are very different from PA features present during winter (not shown). Lau and Nath (1990) point out that summer SSTA patterns exert only a weak influence on the atmosphere. Consequently, the persistence of the PA features in Fig. 1 implies that the winter atmosphere somehow maintains a memory of conditions present during earlier winters. If persistent SSTA patterns contribute to this memory, it will involve the influence of SSTA on synoptic atmospheric variability—that is, changes in the strength of atmospheric storms and the location of the storm track (e.g., Palmer and Sun 1985; Lau and Nath 1990). Regions in which explosive cyclogenesis occurs (e.g., Colucci 1985) may be important in this regard. The influence of a persistent SSTA pattern on atmospheric storms during a given winter could change the preferred locations where blocking patterns tend to form and thus result in regions of anomalously high or low average pressure for that winter (Holopainen 1984; Holopainen and Fortelius 1987; Vautard 1990). Alternatively, the southward propagation of PA features from 1964 to 1984 could suggest a possible connection between climatic variability observed over the Arctic (e.g., Mysak et al. 1990; Ikeda 1990) and the PA features observed over the North Atlantic. Sorting out the responsible mechanisms will require diagnostic studies of the atmospheric reanalysis products currently in production and the analysis of reliable coupled ocean–atmosphere–land–ice models.

Acknowledgments. The support of the National Oceanic and Atmospheric Administration Atlantic Climate Change Program under Grant NA90RAH00075 is gratefully acknowledged. The author acknowledges helpful discussions with H. Bezdek, D. V. Hansen, C. Rooth, and W. Johns.

REFERENCES

- Bjerknes, J., 1964: Atlantic air–sea interaction. *Advances in Geophysics*, Vol. 10, Academic Press, 1–82.
- Cayan, D. A., 1992: Latent and sensible heat flux anomalies over the northern oceans: Driving the sea surface temperature. *J. Phys. Oceanogr.*, **22**, 859–881.
- Colucci, S. J., 1985: Explosive cyclogenesis and large-scale circulation changes: Implications for atmospheric blocking. *J. Atmos. Sci.*, **42**, 2701–2717.
- Delworth, T., S. Manabe, and R. J. Stouffer, 1993: Interdecadal variations of the thermohaline circulation in a coupled ocean–atmosphere model. *J. Climate*, **6**, 141–157.
- Deser, C., and M. L. Blackmon, 1993: Surface climate variations over the North Atlantic Ocean during winter, 1900–1989. *J. Climate*, **6**, 1743–1753.
- Folland, C. K., T. M. Palmer, and D. E. Parker, 1986: Sahel rainfall and worldwide sea temperatures, 1901–85. *Nature*, **320**, 602–606.
- Frankignoul, C., 1985: Sea surface temperature anomalies, planetary waves, and air–sea feedback in the middle latitudes. *Rev. Geophys.*, **23**, 357–390.
- , and R. W. Reynolds, 1983: Testing a dynamical model for midlatitude sea surface temperature anomalies. *J. Phys. Oceanogr.*, **13**, 1131–1145.
- Greatbatch, R. J., and S. Zhang, 1995: An interdecadal oscillation in an idealized ocean basin forced by constant heat flux. *J. Climate*, **8**, 81–91.
- Halliwel, G. R., Jr., and D. A. Mayer, 1996: Frequency response properties of forced climatic SST anomaly variability in the North Atlantic. *J. Climate*, **9**, 3575–3587.
- Hansen, D. V., and H. Bezdek, 1996: On the nature of decadal anomalies in North Atlantic sea surface temperature. *J. Geophys. Res.*, **101**, 8749–8758.
- Holopainen, E., 1984: Statistical local effect of synoptic-scale transient eddies on the time-mean flow in the northern extratropics in winter. *J. Atmos. Sci.*, **41**, 2505–2515.
- , and C. Fortelius, 1987: High-frequency transient eddies and blocking. *J. Atmos. Sci.*, **44**, 1632–1644.
- Hurrell, J. W., 1995: Decadal trends in the North Atlantic oscillation: Regional temperatures and precipitation. *Science*, **269**, 676–679.
- Ikeda, M., 1990: Decadal oscillations of the air–ice–ocean system in the Northern Hemisphere. *Atmos.–Ocean*, **28**, 106–139.
- Kushnir, Y., 1994: Interdecadal variations in North Atlantic sea surface temperature and associated atmospheric conditions. *J. Climate*, **7**, 141–157.
- Lau, N.-C., and M. J. Nath, 1990: A general circulation model study of the atmospheric response to extratropical SST anomalies observed in 1950–79. *J. Climate*, **3**, 965–989.
- Mayer, D. A., and R. H. Weisberg, 1993: A description of COADS surface meteorological fields and the implied Sverdrup transports for the Atlantic Ocean from 30°S to 60°N. *J. Phys. Oceanogr.*, **23**, 2201–2221.
- Mysak, L. A., D. K. Manak, and R. F. Marsden, 1990: Sea-ice anomalies observed in the Greenland and Labrador Seas during 1901–1984 and their relation to an interdecadal Arctic climate cycle. *Climate Dyn.*, **5**, 111–133.
- Palmer, T. N., and Z.-B. Sun, 1985: A modeling and observational study of the relationship between sea surface temperature in the northwest Atlantic and the atmospheric general circulation. *Quart. J. Roy. Meteor. Soc.*, **111**, 947–975.
- Reynolds, R. W., 1979: A stochastic forcing model of sea surface temperature anomalies in the North Pacific and North Atlantic. Climate Research Institute Rep. 8, 31 pp. [Available from College of Oceanic and Atmospheric Sciences, Oregon State University, Corvallis, OR 97331.]
- Vautard, R., 1990: Multiple weather regimes over the North Atlantic: Analysis of precursors and successors. *Mon. Wea. Rev.*, **118**, 2056–2081.
- Wallace, J. M., C. Smith, and C. S. Bretherton, 1992: Singular value decomposition of wintertime sea surface temperature and 500-mb height anomalies. *J. Climate*, **5**, 561–576.
- Weaver, A. J., and E. S. Sarachik, 1991: Evidence for decadal variability in an ocean general circulation model: An advective mechanism. *Atmos.–Ocean*, **29**, 197–231.
- Woodruff, S. D., R. J. Slutz, R. L. Jenne, and P. M. Steurer, 1987: A comprehensive ocean–atmosphere dataset. *Bull. Amer. Meteor. Soc.*, **68**, 1239–1250.
- Zorita, E., V. Kharin, and H. von Storch, 1992: The atmospheric circulation and sea surface temperature in the North Atlantic area in winter: Their interaction and relevance for Iberian precipitation. *J. Climate*, **5**, 1097–1108.